

See discussions, stats, and author profiles for this publication at: <https://www.researchgate.net/publication/19804233>

Pressure-induced dissociation of Brome Mosaic Virus

ARTICLE *in* JOURNAL OF MOLECULAR BIOLOGY · FEBRUARY 1988

Impact Factor: 4.33 · DOI: 10.1016/0022-2836(88)90385-3 · Source: PubMed

CITATIONS

75

READS

16

2 AUTHORS, INCLUDING:



Jerson L Silva

Federal University of Rio de Janeiro

181 PUBLICATIONS 5,131 CITATIONS

SEE PROFILE

Pressure-induced Dissociation of Brome Mosaic Virus

Jerson L. Silva† and Gregorio Weber

Department of Biochemistry, School of Chemical Sciences
University of Illinois, Urbana, IL 61801, U.S.A.

(Received 11 May 1987, and in revised form 31 August 1987)

Brome mosaic virus reversibly dissociates into subunits in the pressure range of 600×10^5 to 1600×10^5 Pa, as demonstrated by studies of the spectral shift of intrinsic fluorescence, of filtration chromatography and of electron microscopy of samples fixed under pressure. Smaller shell particles ($T = 1$) were detected as intermediates in the dissociation pathway. Dissociation was facilitated by decreasing the concentration, as expected for a multimolecular reaction. The estimated change in volume upon dissociation into 90 dimer particles was -2960 ml/mol . Large increases in the intrinsic fluorescence intensity and in the binding of bis(8-anilinonaphthalene-1-sulfonate) occurred at pressures higher than 1400×10^5 Pa. The pressure-dependence profile of the different spectral properties shifted to lower pressures when 5 mM-MgCl₂ was included in the buffer or when the pH was raised from 5.5 to 5.9. When the pressure was progressively increased above 1400×10^5 Pa, a value that led to 75% dissociation, the capsid subunits lost the ability to reassociate into regular shells and only amorphous aggregates were formed after decompression, as evidenced by both electron microscopy and gel filtration chromatography. The formation of these random aggregates of brome mosaic virus can be explained by a conformational drift of the separated subunits, similar in nature to that found in simpler oligomeric proteins.

1. Introduction

Icosahedral viruses are closed protein shells that encapsidate nucleic acids. The degree of complexity varies from viruses containing a single type of subunit to particles made up of many different types of polypeptides. X-ray and electron microscope studies have revealed the unique importance of protein–protein interactions in the formation of icosahedral shells (Harrison, 1983; Rossmann & Erickson, 1985). However, the thermodynamics of subunit association and the mechanism of virus assembly are still very poorly understood. Detailed knowledge of the virus structure does not immediately lead to an explanation of how $60n$ subunits evolve into the assembled virus particle but this puzzle may find its solution in an understanding of the coupling between the subunit association reaction and the first order conformation changes that follow the formation of new subunit contacts. Another intriguing aspect of virus structure is that the number of protein subunits forming the capsid is generally larger than the 60 permitted by icosahedral symmetry. An elegant solution to this problem was formulated by Caspar

& Klug (1962), according to whom the identical protein subunits occupy not equivalent but quasi-equivalent positions in the capsid. Whilst the theory has not been entirely confirmed by high-resolution studies (Rossmann & Erickson, 1985), the concept of triangulation number, the number of subunits that form each of the 60 triangular faces of the icosahedron, has found fruitful application. Hydrostatic pressure can be regarded as a thermodynamic tool, one whose molecular effects depend on the resulting changes in volume, dV , of the system formed by particle plus solvent. The free-energy perturbation $p dV$ displaces the equilibrium in a controlled way. The dissociation of oligomeric proteins by pressure seems to be a general phenomenon (Heremans, 1982; Weber & Drickamer, 1983; Weber, 1987). It can be explained by the imperfect packing of the atoms at the intersubunit surfaces as well as by the hydration accompanied by electrostriction that follows the breaking of intersubunit salt linkages. Virtually all the studies of pressure-induced dissociation of proteins have employed optical methods. Light-scattering is particularly useful when large aggregates are dissociated into many small particles (Payens & Heremans, 1969; Engelborghs *et al.*, 1976) and fluorescence polarization and energy distribution of the fluorescence emission have been used to study the pressure dissociation of small

† Present address: Departamento de Bioquímica, Instituto de Ciencias Biomedicas, Universidade Federal do Rio de Janeiro, 21910 Rio de Janeiro-RJ, Brazil.

oligomers, mostly dimers and tetramers (Paladini & Weber, 1981a; King & Weber, 1986; Silva *et al.*, 1986; Verjovski-Almeida *et al.*, 1986; Royer *et al.*, 1986). More recently, we have developed a system for running polyacrylamide gel electrophoresis under pressures of 1×10^5 to 3000×10^5 Pa (Paladini *et al.*, 1987), permitting the direct demonstration of the pressure dissociating effect.

Here, we describe the effects of hydrostatic pressure (1×10^5 to 3000×10^5 Pa) on the structure of brome mosaic virus (BMV†), an RNA virus formed by the association of 180 copies of a single protein subunit into an icosahedral shell of triangulation number 3 ($T = 3$). Chromatography, electron microscopy and fluorescence were utilized to follow the changes in the virus upon application of pressure.

2. Materials and Methods

(a) Chemicals

Bis-Tris (Ultrol grade) was obtained from Calbiochem. Glutaraldehyde (grade I) was purchased from Sigma Chemical Co. (St Louis, MO), bis-ANS from Molecular Probes (Junction City, OR). All other reagents were of analytical grade. Distilled water was filtered and deionized through a Millipore water purification system to 18-Mohm resistance. Unless stated otherwise, the experiments were performed at 20°C in the standard buffer: 0.05 M-bis-Tris (pH 5.9), 0.5 M-NaCl, 5 mM-MgCl₂.

(b) Virus preparations

BMV was a kind gift from Dr Paul Kaesberg from the University of Wisconsin. BMV was grown on barley plants and was isolated and purified as described (Shih *et al.*, 1972). SV40 was kindly supplied by Dr M. E. Reichmann from the Department of Microbiology at the University of Illinois, R17 phage by Dr D. Beckert from the Massachusetts Institute of Technology. BMV concentration was calculated from the specific absorption ($E_{260} = 5.08 \text{ cm}^2/\text{mg}$ dry weight: Bockstahler & Kaesberg, 1962).

(c) Fluorescence studies under pressure

The high-pressure bomb has been described by Paladini & Weber (1981a,b). Fluorescence spectra were recorded on a microprocessor-controlled, photon counting, scanning spectrophotometer (Royer, 1985). The spectra were corrected for wavelength response of the phototube and monochromator. Fluorescence spectra at pressure p were quantified by the specification of the center of spectral mass, $\langle v_p \rangle$

$$\langle v_p \rangle = \sum \bar{v}_i F_i / \sum F_i \quad (1)$$

where F_i is the fluorescence emitted at wavenumber \bar{v}_i and the summation is carried out over the range of

appreciable values of F . The degree of dissociation (a_p) is related to $\langle v_p \rangle$ by the expression:

$$a_p = (1 + Q(\langle v_p \rangle - \langle v_F \rangle)) / (\langle v_I \rangle - \langle v_F \rangle))^{-1}, \quad (2)$$

where Q is the ratio of the quantum yields of dissociated and associated forms, $\langle v_p \rangle$ is the center of spectral mass at pressure P , and $\langle v_F \rangle$ and $\langle v_I \rangle$ are the corresponding quantities for dissociated and associated forms (Paladini & Weber, 1981a; Silva *et al.*, 1986). The importance of the characterization of the spectral displacements by the mean wavenumber of the emission (eqn (1)) rather than by the change of the maximum of emission should be stressed. The latter is a differential quantity and the precision with which it is determined does not usually exceed 1 nm. The center of mass is an integral measure that can reach a precision of $\pm 10 \text{ cm}^{-1}$. In a heterogeneous system, e.g. the tryptophan residues of a protein molecule, considerable displacements of the center of mass can take place with small or imperceptible changes in the maximum of emission.

(d) Electron microscopy of samples fixed under pressure

A Jeol 100 CX electron microscope was used for observation of the samples. Negative staining was performed with ammonium molybdate or uranyl acetate. In order to observe the ultrastructure of BMV under pressure, we developed a simple method for fixing the sample with glutaraldehyde under a desired pressure. For this purpose, we used the pressure bomb described by Paladini & Weber (1981b) with a modified sample container. The bottle-shaped sample cell was made of glass and had 2 adjacent compartments, one for the sample and one for a 0.5% glutaraldehyde solution, separated by a vertical partition that did not reach the neck of the bottle. Dodecane was used to fill the cell above the surfaces of the sample and glutaraldehyde solutions in the 2 compartments, and within the compressible plastic cap. During an experiment, the BMV sample was subjected to pressure for 45 min to 1 h and mixing under pressure was then performed by inverting and shaking the bomb for about 5 min. All other apparatus were as described for the spectroscopic experiments.

(e) Size exclusion high-pressure liquid chromatography

This was performed in a prepacked SynChropak GPC500 column of 250 mm \times 4.6 mm internal diameter, obtained from SynChrom, Inc. (Linden, NJ). Typically, a flow-rate of 0.3 ml/min was used. Elution of the sample was monitored by absorption or fluorescence. The void volume (V_0) of the column was measured with lambda phage DNA and the total volume (V_t) with ADP. Calibration of the column was performed using viruses of different sizes: satellite tobacco necrosis viruses (STNV), R17 phage, BMV and SV40. The partition coefficient k_d was calculated employing the relation: $K_d = (V_E - V_0) / (V_t - V_0)$, where V_E is the elution volume of the virus. The partition coefficients are plotted against the hydrodynamic radii of the viruses in Fig. 7.

3. Results

(a) Spectroscopic studies

The effects of pressure on BMV were initially examined by measuring spectral distributions of

† Abbreviations used: BMV, brome mosaic virus; bis-Tris, {[bis-(2-hydroxyethyl)-imino]-tris(hydroxymethyl)methane}; bis-ANS, bis(8-anilinonaphthalene-1-sulfonate); SV40, simian virus 40; STNV, satellite tobacco necrosis virus.

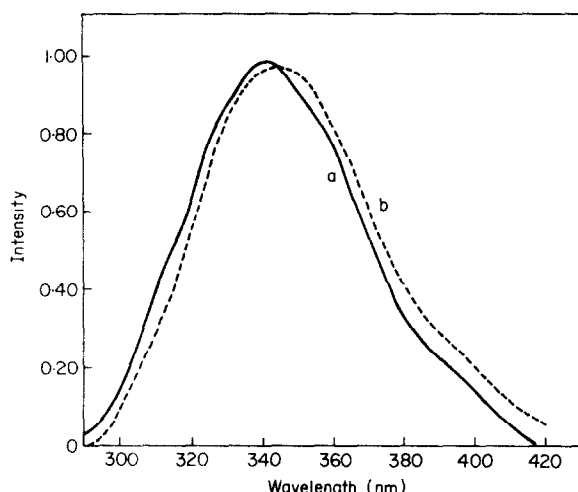


Figure 1. Intrinsic fluorescence spectra of BMV (60 µg/ml) at (a) atmospheric pressure and (b) at 1750×10^5 Pa, excited at 280 nm, in 0.05 M-bis-Tris, 0.5 M-NaCl, 5 mM-MgCl₂ at pH 5.9. The temperature was 20°C.

intrinsic fluorescence. Figure 1 shows spectra of the intrinsic fluorescence of a buffer solution (pH 5.9) containing 60 µg of BMV/ml at atmospheric and at high pressure (1750×10^5 Pa). Up to 1600×10^5 Pa, the spectral changes were reversible after release of pressure. Spectral shifts were quantified as changes in the average energy of emission $\langle \bar{v} \rangle$, as described in Materials and Methods. Figure 1 shows a red shift of the emission of 300 cm^{-1} . The simplest interpretation of the red shift is that at high pressures one or more intrinsic fluorophores becomes exposed to a medium of increased polarity, presumably water. Figure 2 shows plots of $\langle \bar{v} \rangle$ and of the total intrinsic fluorescence intensity against pressure, in the absence (filled symbols) and in the presence (open symbols) of 5 mM-magnesium. The pressure-dependent profiles of both spectral properties shifted to lower pressures when 5 mM-MgCl₂ was added to the medium. In both conditions, the increase in fluorescence intensity occurred at distinctly higher pressures than the decrease in

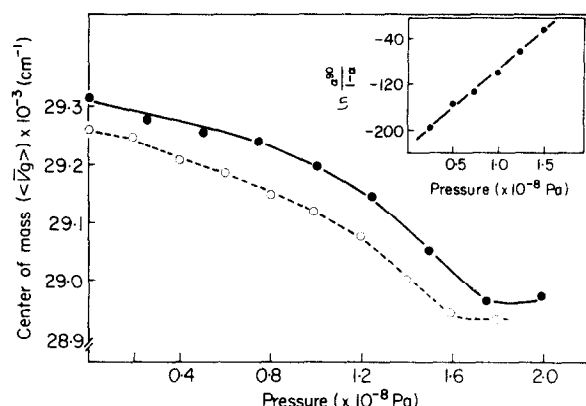


Figure 3. Concentration dependence of the spectral changes induced by pressure. Plot of center of spectral mass *versus* pressure at 2 concentrations, 60 µg BMV/ml (●) and 10 µg BMV/ml (○). Other conditions as for Fig. 1. Inset: plot of $\ln(a^{90}/1-a)$ *versus* pressure at 60 µg BMV/ml.

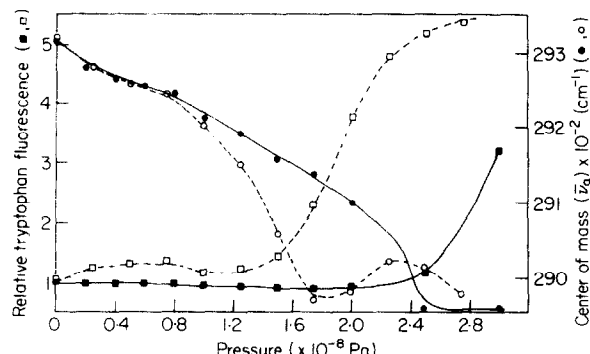
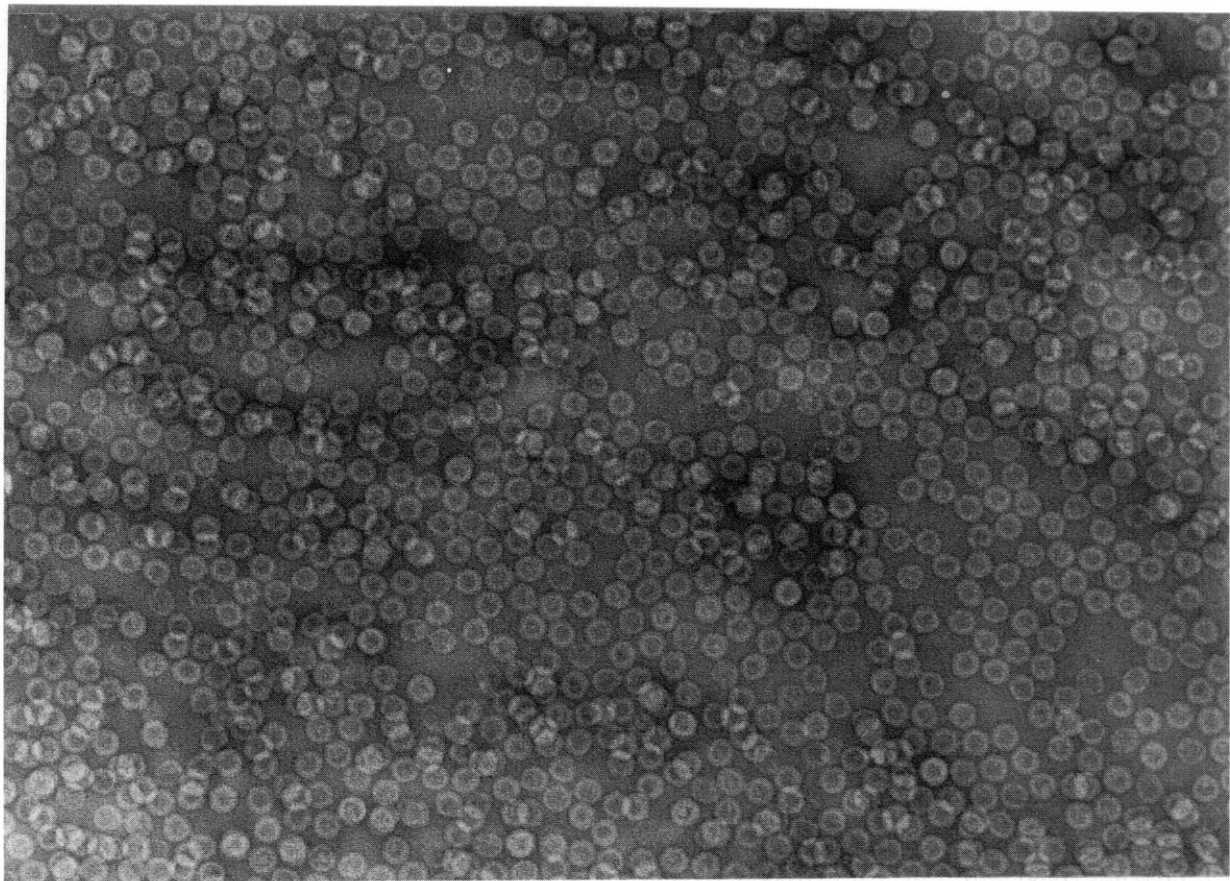


Figure 2. Plot of center of spectral mass (○, ●) and intensity of intrinsic fluorescence (□, ■) *versus* pressure, in the absence (●, ■) and in the presence (○, □) of 5 mM-magnesium. Other conditions as for Fig. 1.

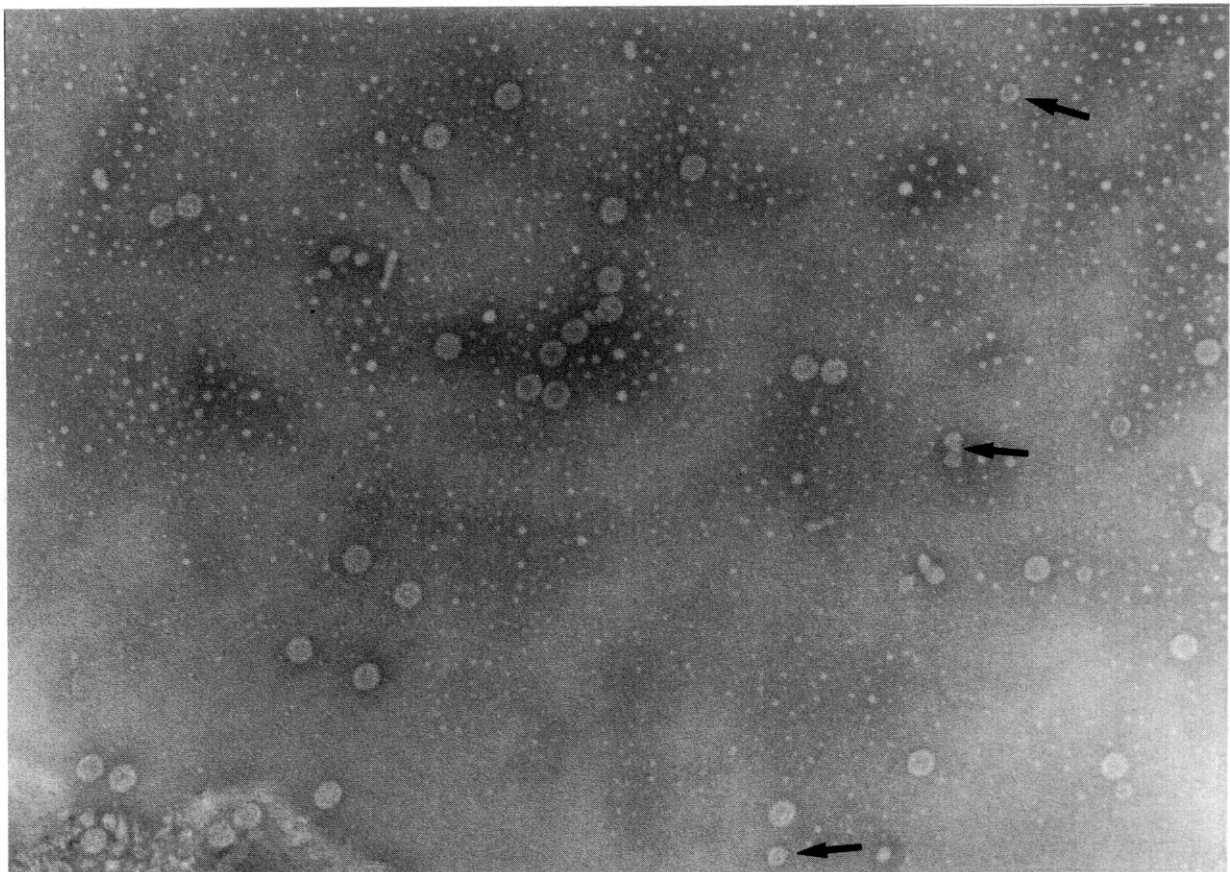
center of mass. The fluorescence intensity changes became progressively irreversible as the pressures approached the curve plateau. A red shift of the intrinsic fluorescence of an oligomeric protein can conceivably occur either by changes in the tertiary conformation or by dissociation but the former effect has been found only at pressures higher than 5000×10^5 Pa (Li *et al.*, 1976; Weber & Drickamer, 1983). The spectral shifts in BMV fluorescence occur in a much lower pressure range, the same in which shifts corresponding to authentic dissociation of dimers (Paladini & Weber, 1981a; Silva *et al.*, 1986) and tetramers (King & Weber, 1986; Royer *et al.*, 1986) takes place. It does seem to indicate a dissociation reaction. More direct information about the source of the spectral shift can be obtained by a study of the dependence upon protein concentration: a dissociation process must occur more readily as the total protein concentration is decreased, whereas a tertiary conformational change, a typical first-order reaction, is concentration independent. In Figure 3, the dependence on BMV concentration of the change of center of spectral mass upon pressure was tested. The pressure at mid-dissociation ($p_{1/2}$) was 170×10^5 Pa smaller for the sixfold lower BMV concentration, consistent with a dissociation reaction. For dissociation of a whole virus, it is not possible to determine the change in $p_{1/2}$ expected for a given decrease of protein concentration, because the order and pathway of the reaction is unknown. We found that the fluorescence intensity changes induced by pressure were less dependent on protein concentration (data not shown).

(b) Electron microscopy

Direct evidence for pressure-induced dissociation of BMV to small particles was obtained by transmission electron microscopy. The system devised to fix the sample with glutaraldehyde under pressure is described in Materials and Methods.

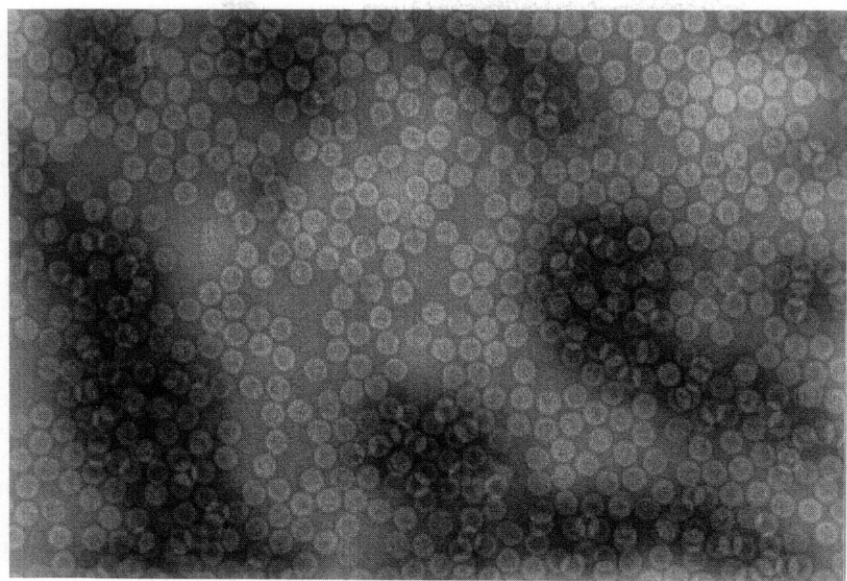


(a)

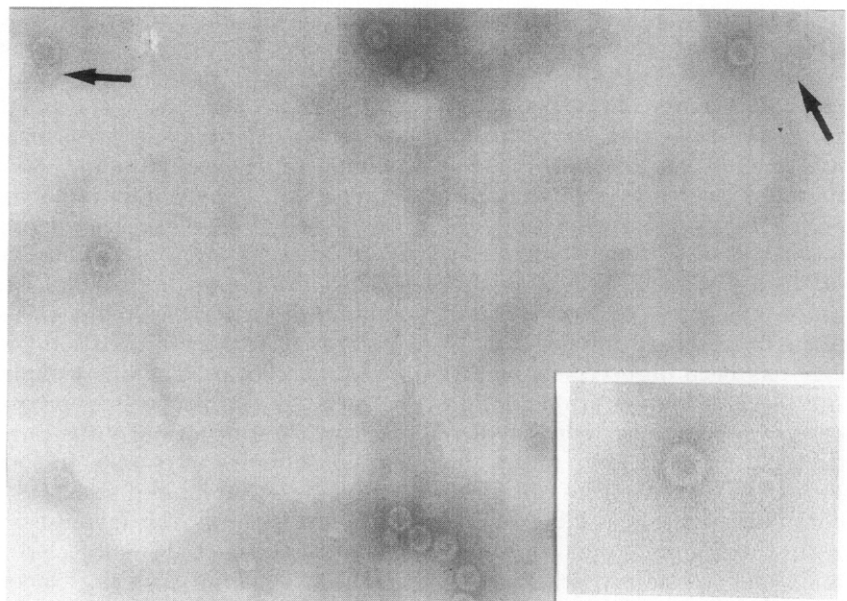


(b)

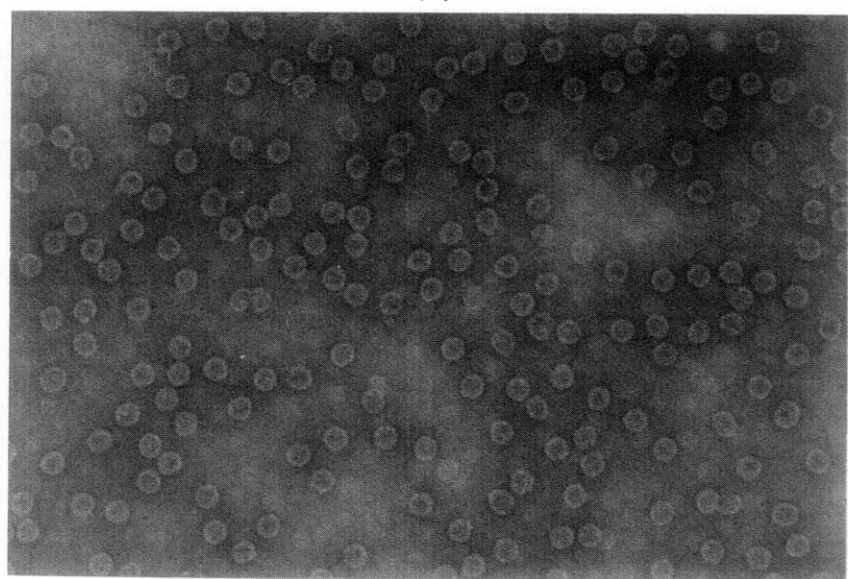
Figure 4. Electron microscopy of BMV fixed under pressure. BMV (0.2 ml of 60 µg/ml) was mixed with an equal volume of 0.5% glutaraldehyde solution as described in Materials and Methods. BMV sample was fixed after 45 min incubation at (a) atmospheric pressure and (b) under 1400×10^5 Pa. Magnification 172,000 \times . All other conditions as described for Fig. 1.



(a)



(b)



(c)

Figure 5. Electron microscopy of BMV fixed under 1400×10^5 Pa and after release of pressure. Conditions as for Fig. 4, except that BMV was fixed after 1 h incubation at (a) atmospheric pressure (b) under 1400×10^5 Pa and (c) after release of pressure. Magnification $160,000\times$. Inset: comparison of $T = 3$ and $T = 1$ particles; magnification $260,000\times$.

Figure 4 shows electron micrographs of BMV samples fixed after incubation for 45 min at (a) atmospheric pressure or (b) under 1400×10^5 Pa. In Figure 5, the incubation time was one hour and fixation with glutaraldehyde was performed at (a) atmospheric pressure, (b) under 1400×10^5 Pa or (c) initiated within a few seconds after the restoration of atmospheric pressure. The dramatic decrease in the number of particles at 1400×10^5 Pa demonstrates that most of the virus capsids undergo dissociation (Fig. 5(b) and (c)) into smaller units, which are not resolved by the microscope. We stress that the micrographs shown were typical for the whole grid. Similar results were obtained when uranyl acetate was used instead of ammonium molybdate. Figure 5(c) shows that great numbers of subunits reassociated rapidly to $T = 3$ capsids following restoration of atmospheric pressure after being subjected to 1400×10^5 Pa, thus indicating the reversibility of the dissociation reaction at 1400×10^5 Pa. It should be noted that at 1400×10^5 Pa the change in center of spectral mass was already large, whereas the tryptophan fluorescence intensity was not yet affected (Fig. 2). The electron micrographs therefore reinforce the hypothesis that the spectral shift is correlated with the virus dissociation, whilst the changes in intensity correspond to a direct effect of pressure upon the fluorescence efficiency of tryptophan. Indeed, the change in fluorescence intensity with pressure in this range has been observed in single-chain proteins (Li *et al.*, 1976). Figures 4(b) and 5(b) show also the presence of spherical particles smaller than the original BMV. Their size (inset in Fig. 5(b)) is similar to the $T = 1$ particles obtained by treatment of BMV with trypsin (Cuillel *et al.*, 1981). The arrows in the Figure point to some $T = 1$ particles and one structure where the splitting of $T = 3$ to $T = 1$ shells seems to be occurring. These results indicate that pressure dissociation of BMV occurs with the intermediate formation of at least some $T = 1$ particles.

We found that as the pressure of incubation was increased the recovery of virus structures decreased. When BMV was subjected to 2200×10^5 Pa, the recovery of shell structures was very small (Fig. 6) in comparison to the experiment shown in Figure 5(c) (1400×10^5 Pa). In addition to a decrease in the particle number, larger shells and gelled material that probably results from the random aggregation of altered subunits can be observed (Fig. 6). The appearance of this gelled material accounts for the irreversibility of the spectroscopic parameters when these higher pressures are attained.

(c) Sizing chromatography of BMV

High-pressure liquid chromatography was utilized to size the virus particles and sub-particles within ten to 15 minutes after release of pressure. The sizing column was calibrated with four viruses encompassing the range of shell radius between 80

and 250 Å (Fig. 7: $1 \text{ \AA} = 0.1 \text{ nm}$). The elution position of BMV detected by its absorbance at 260 nm agrees very well with that expected for a hydrodynamic particle of 280 Å diameter (Fig. 7). In Figure 8 the tryptophan fluorescence was used to monitor the elution of BMV from the column after incubation for one hour at atmospheric pressure (Fig. 8(a)) or at 1600×10^5 Pa (Fig. 8(b) and (c)). The sample was applied to the column one minute (Fig. 8(b)), or 20 minutes (Fig. 8(c)) after release of pressure and all the peaks were read within 12 minutes. In addition to the tallest peak, corresponding in each panel to the native virus, two extra peaks appeared after pressure treatment. The more included peak eluted in the total volume and amounted to 50% of the protein. Presumably, it corresponds to dissociated capsid protein. The GPC500 column totally includes proteins smaller than 50,000 M_r . So, the dissociated peak may correspond to dimers ($M_r = 40,000$) or monomers ($M_r = 20,000$). It is noteworthy that no material elutes between the virus and the dissociated protein peaks. The more excluded peak eluted in the void volume of the column and was enriched at the expense of the dissociated protein as time progressed (Fig. 8(c)). The aggregate formed is at least twice as large as the native BMV, since the exclusion limit of this column is about 300 Å. The amount of virus recovered decreased as the pressure was raised, and the incubation time was lengthened (data not shown). The likely explanation is that the dissociated capsid protein progressively loses the ability to form normal virus particles. The altered capsid subunits were able to form only unspecific aggregates of unlimited size.

Figure 9 shows the increase in susceptibility to ribonuclease of BMV subjected to high pressure. BMV (60 µg/ml) was incubated with a concentration of RNase (0.3 µg/ml) that caused no digestion even after 24 hours at atmospheric pressure. When BMV in the presence of RNase was subjected to 1800×10^5 Pa, a large amount of hydrolysis occurred, as shown by the appearance of nucleic acid fragments eluting close to the total volume. These data give additional support to the dissociating effect of pressure on BMV.

(d) Bis-ANS binding to BMV

The fluorescence yield of bis(8-anilinonaphthalene-1-sulfonate) increases up to 100-fold when it is transferred from water to a non-polar environment, as may occur in binding to hydrophobic domains in proteins (Rosen & Weber, 1969). When a protein is partially or completely disorganized, hydrophobic segments may be exposed. Bis-ANS binding to intact BMV at 10^5 Pa was not detected. It was also insignificant at 1400×10^5 Pa, when extensive dissociation had already occurred (Fig. 2). Binding of bis-ANS occurred only when BMV was subjected to pressures in the same range as those that cause an

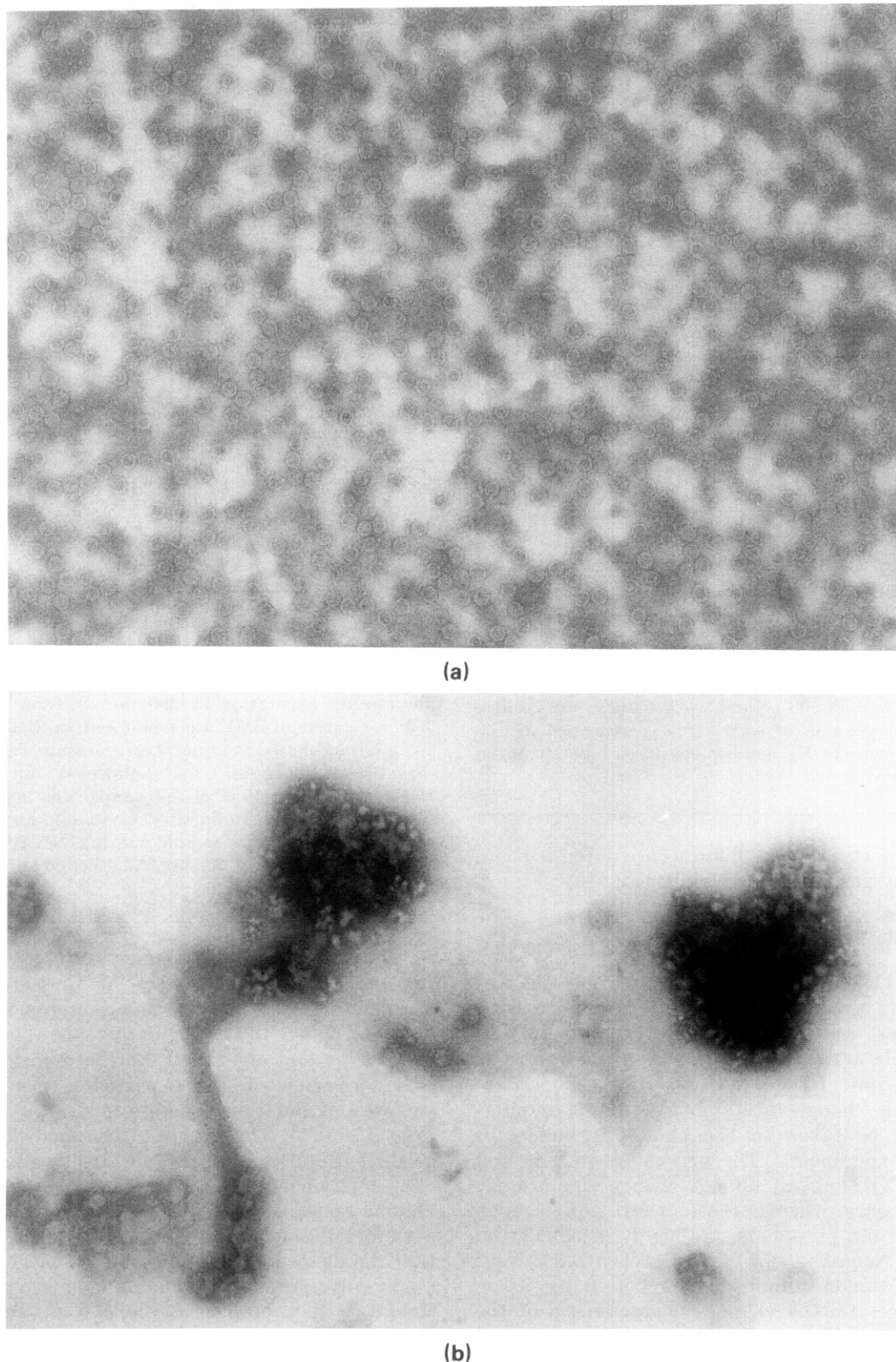


Figure 6. Electron microscopy of BMV fixed after release of pressure 2200×10^5 Pa: (a) 1 h incubation at atmospheric pressure; (b) 1 h incubation at 2200×10^5 Pa and fixed after release of pressure. Magnification $106,400\times$.

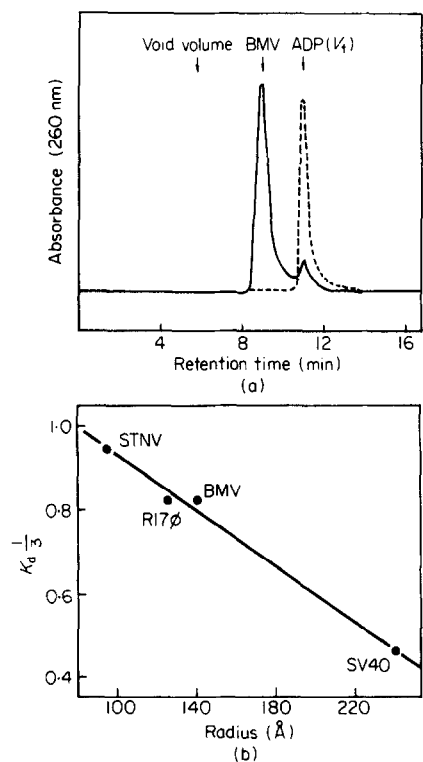


Figure 7. Size exclusion high-pressure liquid chromatography of BMV. (a) The 260 nm absorption elution of BMV from the GPC500 column eluted with 0.05 M-bis-Tris, 0.5 M-sodium acetate and 5 mM-magnesium acetate at pH 5.9. The flow-rate was 0.3 ml/min. (b) Calibration curve for the GPC500 column with icosahedral viruses. The elution position of each virus is expressed as the partition coefficient K_d , and is plotted as a function of the known radius.

increase in tryptophan fluorescence intensity and accompany general irreversibility (Fig. 10).

(e) pH dependence of pressure-induced changes

Figure 11 shows that the spectroscopic changes induced by pressure are facilitated by increasing pH. It has been shown repeatedly that BMV is more stable at the lower pH values (Incardona & Kaesberg, 1964; Pfeiffer & Hirth, 1974; Cuillel *et al.*, 1983). This change in stability with pH requires that care be taken in the choice of buffer for pressure experiments. The pK values of Tris and bis-Tris (NH buffers) do not change significantly under pressure, whereas those of OH buffers, such as acetate and phosphate, are highly dependent on pressure (Neuman *et al.*, 1973). When 0.5 M-NaCl from the standard buffer was replaced by 0.5 M-sodium acetate, the changes characteristic of the dissociation of BMV by pressure were not observed even at pressures of 2200×10^5 Pa (data not shown).

4. Discussion and Conclusions

The main goal of this study was to use hydrostatic pressure to approach the problems of protein-protein interactions in the assembly of

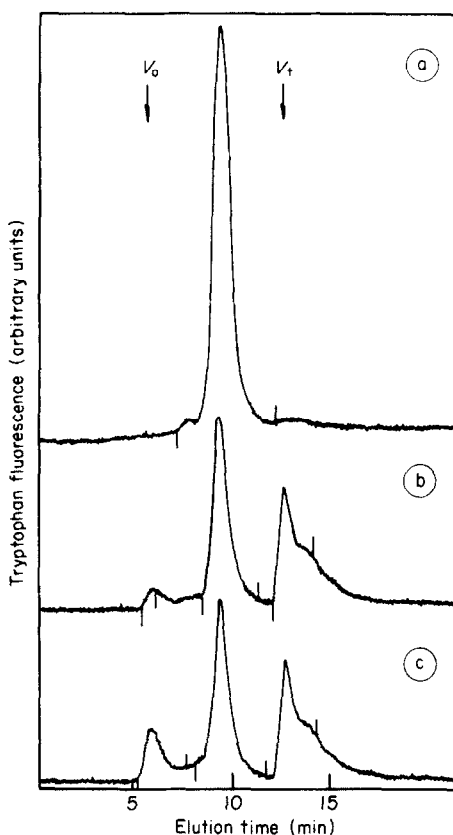


Figure 8. Size exclusion high-pressure liquid chromatography of BMV after pressure treatment. The intrinsic fluorescence (excitation at 290 nm, emission at 320 to 360 nm) elution of BMV was monitored. (a) BMV (50 µl of 60 µg/ml) incubated at atmospheric pressure was injected. (b) BMV (60 µg/ml) was subjected for 1 h to 1600×10^5 Pa and 50 µl of the sample was injected into the GPC500 column 1 min after release of pressure. (c) As in (b), except that the sample was injected 20 min after return to atmospheric pressure. All other conditions as for Fig. 7.

icosahedral viruses. We demonstrate for the first time the dissociating effect of pressure on an icosahedral virus. Brome mosaic virus was fully dissociated by 1600×10^5 Pa, in the presence of magnesium and at pH 5.9. Furthermore, we found that formation of $T = 1$ particles occurs in the pathway of BMV disassembly induced by pressure (Figs 4 and 5). The nature of the final dissociated product is not known precisely. It has a low degree of association as judged from its elution in the total volume of the size exclusion column (Fig. 8). The asymmetric elution from the column also indicates that the dissociated protein is not homogeneous. It might correspond to a dimer-monomer equilibrium similar to that obtained by Cuillel *et al.* (1983) when BMV capsid protein was kept at high pH.

The effects on BMV structure observed under pressure do not seem to be restricted to dissociation. At least two different processes are occurring. The processes that take place in a lower pressure range (1600×10^5 Pa, in the presence of Mg) are related to the reversible breakdown of the virus structure as evidenced by electron microscopy

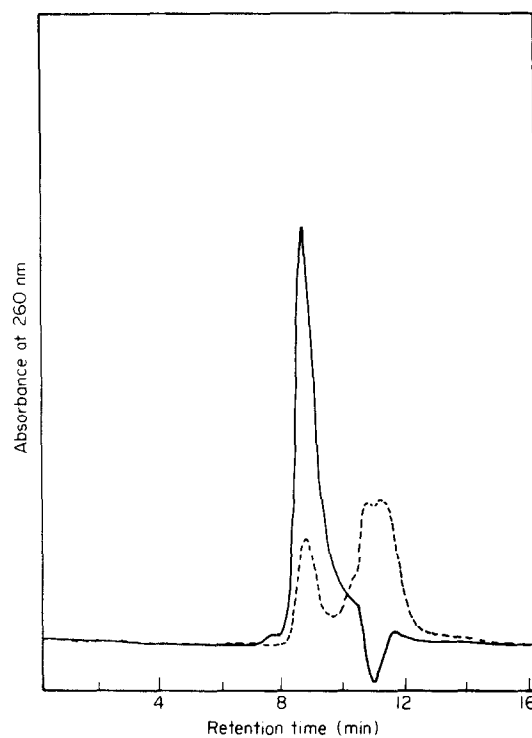


Figure 9. Susceptibility of BMV to RNase. BMV (60 µg/ml) was incubated with 0.3 µg RNase/ml for 30 min. either at atmospheric pressure (—) or 1800×10^5 Pa (---); 50 µl of the sample was injected into the GPC500 column 1 to 3 min after release of pressure, and absorbance at 260 nm was monitored. All other conditions as for Figure 7.

(Figs 4 and 5) and the red shift of the tryptophan emission. In this pressure range, it is possible to recover on decompression a significant proportion of the original structure as judged by fluorescence, size chromatography and electron microscopy.

Ordinarily, the pressure dissociation data permit the calculation of thermodynamic parameters related to the subunit association reaction; namely, the dissociation constant at atmospheric pressure and the standard volume change of association

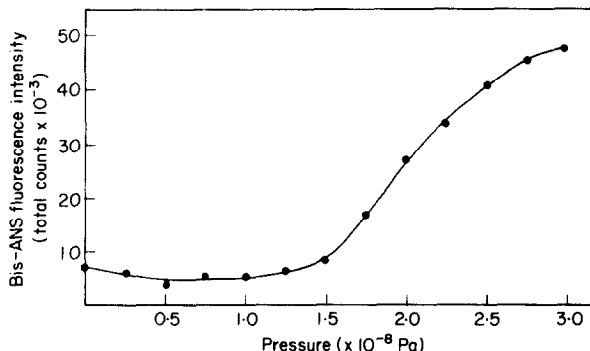


Figure 10. Effect of pressure on binding of bis-ANS to BMV. The bis-ANS fluorescence (excitation at 360 nm, emission at 400 to 540 nm) was measured as a function of pressure. BMV concentration was 60 µg/ml; the bis-ANS concentration was 2 µM. All other conditions as for Fig. 1.

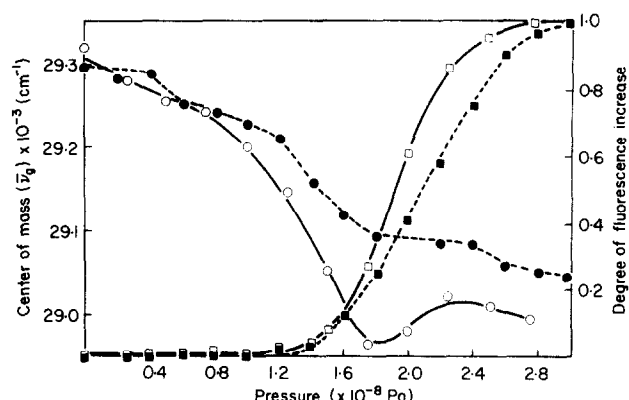


Figure 11. Effect of pH on pressure dissociation of BMV. Plot of center of spectral mass (○, ●) and intensity of intrinsic fluorescence (□, ■) versus pressure. The continuous lines are for pH 5.9 (○, □) and the broken lines are for pH 5.5 (●, ■). The virus concentration was 60 µg/ml. Other conditions as for Fig. 1.

(Paladini & Weber, 1981a,b; Weber & Drickamer, 1983; Silva *et al.*, 1986). The dissociation constant cannot be calculated for the pressure dissociation of BMV, because the pathway of dissociation is not completely known, but the total volume change on association can be estimated in the following manner. On account of the limited precision of the measurements, it is convenient to employ an integrated expression relating the change in equilibrium constant to the finite increment in pressure above atmospheric pressure (Paladini & Weber, 1981a):

$$\ln (K_p/K_0) = pdV^0/RT, \quad (3)$$

where K_p and K_0 are the dissociation constants at pressures p and atmospheric, respectively. If the association reaction consists in the association of n particles, and there are no appreciable amounts of reaction intermediates:

$$K_p = a_p^n C^{n-1} / (1 - a_p); K_0 = a_0^n C_{n-1} / (1/a_0), \quad (4)$$

where a_p and a_0 are the degree of dissociation at pressure p and atmospheric, respectively, and C is the total particle concentration expressed as associated species.

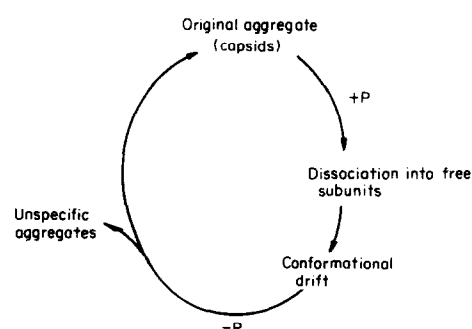


Figure 12. Diagram for the dissociation and conformational drift of BMV.

From the last two equations:

$$pdV^0/RT = \ln[a_p^n/(1-a_p)] - \ln[a_0^n/(1-a_0)] \quad (5)$$

or

$$pdV^0/RT = \ln[a_p^n/(1-a_p)] - \text{constant}. \quad (6)$$

The inset in Figure 3 shows a logarithmic plot against pressure according to the last equation. From it, dV^0 for the association of the whole virus was calculated to be 2960 ml mol^{-1} , corresponding to dV^0 of 66 ml mol^{-1} per particle. Although equation (5), which treats the association as a reaction of order 90 may appear as somewhat arbitrary, it is important to notice that the above value of 66 ml mol^{-1} per particle obtained by its means is of the same order as that observed for protein dimers, 30 ml for yeast enolase (Paladini & Weber, 1981a), 75 ml for tryptophan synthase (Silva *et al.*, 1986), and for tetramers, 60 mol mol^{-1} for porcine lactate dehydrogenase (King & Weber, 1986). The similarity of these figures points, also for the virus, to a contribution from salt linkages between the subunits. The importance of electrostatic forces for the stabilization of subunit–subunit interactions in icosahedral viruses has been pointed out repeatedly (Hsu *et al.*, 1976; Raymet *et al.*, 1979; Rossmann *et al.*, 1983; Rossmann & Erickson, 1985).

The further processes that occur at pressures higher than $1400 \times 10^5 \text{ Pa}$ are revealed by an increase of tryptophan fluorescence quantum yield (Figs 2 and 11) and by binding of bis-ANS (Fig. 10). Beyond this pressure, the recovery of the original state is progressively less complete as the pressure is raised and the incubation time is lengthened. The processes that occur in the low and high-pressure ranges are correlated with each other, since they are favored by the same conditions (absence of magnesium and increase of pH). The size exclusion chromatography experiments illustrated by Figure 8 are particularly important to clarify the nature and coupling of the phenomena in the "low" and "high" pressure ranges. In experiments carried out under conditions ($1600 \times 10^5 \text{ Pa}$, pH 5.9 and 5 mM-MgCl_2) that correspond to the top of the low pressure range and the beginning of the high range, injection of the sample into the size column immediately after decompression led to approximately 50% of the protein being eluted in the dissociated form and about 5% of the protein eluted in a non-specific aggregated form. At longer intervals after release of pressure, part of the dissociated protein aggregated, increasing the amount of protein fluorescence eluting in the void volume of the column. Amorphous aggregates were also observed in the electron micrographs of BMV subjected to $2200 \times 10^5 \text{ Pa}$ (Fig. 6). Pfeiffer & Hirth (1974) also obtained amorphous aggregates after reversal of acidic and low ionic conditions that had promoted virus capsid dissociation. It can be concluded that a fraction of the protein reassociated to form native-like virus capsids, whilst another fraction lost this ability and was able to form only

amorphous aggregates. These phenomena are similar in nature to those found with simple oligomeric proteins, in which we observed a loss of free energy of association of the subunits when these became separated following changes in concentration (Xu & Weber, 1982), pressure (King & Weber, 1986; Silva *et al.*, 1986) and temperature (King & Weber, 1986). We have concluded that the observed effects result from slow changes in the conformation of the dissociated subunits that take place when they become separated from each other, regardless of the cause of separation. The loss of contacts between the subunits results in changes in their conformation so that an aggregate of diminished subunit affinity is formed when the particles eventually reassociate. Various observations (see summary by Weber, 1987) indicate that this loss of affinity and the concomitant changes in enzyme activity and spectral characteristics are time-dependent phenomena that evolve independently of each other so that the separated subunits exist in a variety of time-dependent conformations. Accordingly, we postulate the existence of a "conformational drift" that follows subunit separation. It seems likely that when dissociation of the virus is carried almost to completion, the subunits remain separated for a time sufficiently long for them to undergo a conformational drift important enough to prevent proper association upon decompression. The incomplete recovery of the virus as the pressure is raised and the time of high-pressure incubation is lengthened is entirely similar to that seen with the enzymatic activity of lactate dehydrogenase (King & Weber, 1986): the longer the time that the subunits are kept apart, the longer the conformational drift and the more lengthy and difficult the process of recovery of the initial properties. The scheme described in Figure 12 would apply to lactate dehydrogenase as well as to brome mosaic virus.

Rossmann & Erickson (1985) have emphasized the importance of tertiary and quaternary structural changes during the assembly of icosahedral viruses. They suggest that the association of a limited number of subunits may alter their relationships to subsequent subunit additions. Thermodynamically, this can be accomplished only if the free energy change of association decreases during the assembly reaction. Reciprocally, we expect that during the disassembly reaction the subunit affinity decreases depending upon the extent of dissociation as proposed by the conformational drift hypothesis (Weber, 1986). Our results point out to the presence of a highly "drifted" subunit population that is unable to form virus capsids. It should be pointed out that this population is obtained only at high degrees of dissociation as expected by the conformational drift hypothesis (Weber, 1986; Silva *et al.*, 1986). The identification of specific conditions that can recover the capsid assembly ability of this population should prove an interesting subject for further studies.

We are grateful to Dr E. Basgall from the Electron Microscopy Center at the University of Illinois for his generous collaboration and use of his facilities for electron microscopy. We are also grateful to Dr P. KAESBERG from the University of Wisconsin for providing BMV.

The work was supported by a grant from the National Institutes of Health (GM11223) to G.W. J.L.S. was partly supported by a post-doctoral fellowship award from the Conselho Nacional de Desenvolvimento Científico e Tecnológico (CNPq) of Brazil.

References

- Bockstahler, L. E. & KAESBERG, P. L. (1962). *Biophys. J.* **2**, 1-9.
- Casper, D. L. D. & Klug, A. (1962). *Cold Spring Harbor Symp. Quant. Biol.* **27**, 1-24.
- Cuillel, M., Jacrot, B. & Zulauf, M. (1981). *Virology*, **110**, 63-72.
- Cuillel, M., Zulauf, M. & Jacrot, B. (1983). *J. Mol. Biol.* **164**, 589-603.
- Engelborghs, Y., Heremans, K. A., De Maeyer, L. & Hoebeke, J. (1976). *Nature (London)*, **256**, 686-689.
- Harrison, S. C. (1983). *Advan. Virus Res.* **28**, 175-240.
- Heremans, K. A. (1982). *Annu. Rev. Biophys. Bioeng.* **11**, 1-21.
- Hsu, C. H., Sehgal, O. P. & Pickett, E. E. (1976). *Virology*, **69**, 587-595.
- Incardona, N. L. & KAESBERG, P. (1964). *Biophys. J.* **4**, 11-21.
- King, L. & Weber, G. (1986). *Biochemistry*, **25**, 3632-3637.
- Li, T. M., Hook, J. W., III, Drickamer, H. G. & Weber, G. (1976). *Biochemistry*, **15**, 5571-5580.
- Neuman, R. C., Kauzmann, W. & Zipp, A. (1973). *J. Phys. Chem.* **77**, 2687-2691.
- Paladini, A. A. & Weber, G. (1981a). *Biochemistry*, **20**, 2587-2593.
- Paladini, A. A. & Weber, G. (1981b). *Rev. Sci. Instrum.* **52**, 419-427.
- Paladini, A. A., Silva, J. L. & Weber, G. (1987). *Anal. Biochem.* **161**, 358-364.
- Payens, T. A. J. & Heremans, K. A. H. (1969). *Biopolymers*, **8**, 335-345.
- Pfeiffer, P. & Hirth, L. (1974). *Virology*, **61**, 160-167.
- Rayment, I., Johnson, J. E. & Rossmann, M. G. (1979). *J. Biol. Chem.* **254**, 5243-5245.
- Rosen, C.-G. & Weber, G. (1969). *Biochemistry*, **8**, 3915-3920.
- Rossmann, M. G. & Erickson, J. W. (1985). In *Virus Structure and Assembly* (Casjens, S., Ed.), pp. 29-73. Jones & Batlett Publishers, Inc., Boston.
- Rossmann, M. G., Abad-Zapatero, C., Hermodson, M. A. & Erickson, J. W. (1983). *J. Mol. Biol.* **166**, 37-83.
- Royer, C. A. (1985). Ph.D. dissertation, University of Illinois at Urbana-Champaign, Urbana, IL.
- Royer, C. A., Weber, G., Daly, T. J. & Matthews, K. S. (1986). *Biochemistry*, **25**, 8308-8315.
- Shih, D., Lane, L. & KAESBERG, P. (1972). *J. Mol. Biol.* **64**, 353-362.
- Silva, J. L., Miles, E. W. & Weber, G. (1986). *Biochemistry*, **25**, 5780-5786.
- Verjovski-Almeida, S., Kurtenbach, E., Amorim, A. F. & Weber, G. (1986). *J. Biol. Chem.* **261**, 9872-9878.
- Weber, G. (1986). *Biochemistry*, **25**, 3626-3631.
- Weber, G. (1987). In *High Pressure Chemistry and Biochemistry* (van Eldyk, R. & Jonas, J., eds), NATO ASI Ser. Math. Phys. Sci., vol. 197, pp. 401-420. Reidel, Dordrecht.
- Weber, G. & Drickamer, H. G. (1983). *Quart. Rev. Biophys.* **116**, 89-112.
- Xu, G.-J. & Weber, G. (1982). *Proc. Nat. Acad. Sci., U.S.A.* **79**, 5268-5271.

Edited by P. H. von Hippel